

## Electromagnetic absorption for a superconductor with states in the gap

W. Stephan and J. P. Carbotte

*Physics Department, McMaster University, Hamilton, Ontario, Canada L8S 4M1*

(Received 23 October 1985)

We have calculated the electromagnetic absorption of superconducting alloys containing paramagnetic impurities in the model of Shiba and Rusinov. A peak in the absorption is found to appear at low frequencies and finite temperatures, the temperature variation of which may be useful in determining appropriate phase shifts for particular alloys. The absorption is calculated for Pb-Mn and Zn-Mn alloys using scattering phase shifts derived from tunneling experiments. In the case of Pb-Mn, only one of the two candidate parameter sets is found to be consistent with existing experimental results.

### I. INTRODUCTION

The absorption of electromagnetic radiation is one of the more direct probes of the details of the electronic quasiparticle density of states of a superconductor, providing the same type of information as the more common tunneling experiments. The far-infrared study by Dick and Reif<sup>1</sup> of Pb-Gd alloy films provided corroboration of the applicability of the theory of Abrikosov and Gor'kov<sup>2</sup> (AG) to these alloys, in agreement with the results of tunneling experiments by Woolf and Reif.<sup>3</sup> These same experiments also showed convincingly that Pb-Mn alloys are not well described by AG theory.

Chaba and Nagi<sup>4</sup> have reexamined the tunneling conductance of these Pb-Mn alloys using the theory of Shiba<sup>5</sup> and Rusinov<sup>6</sup> (SR). SR theory, which is believed to be a significantly better approximation than AG theory when coupling between conduction electrons and localized impurity spins is large, was found to give better agreement with the Pb-Mn tunneling characteristics than does AG theory. Machida<sup>7</sup> has examined the electromagnetic absorption experiments on Pb-Mn films using SR theory and also found better agreement than was found with AG theory.

The analyses of Machida<sup>7</sup> and Chaba and Nagi<sup>4</sup> both employed only contributions from *S*-wave scattering in the summation over partial waves which appears in SR theory. Tsang and Ginsberg<sup>8</sup> have also performed tunneling experiments on Pb-Mn alloys, and have examined their results in terms of three partial waves in SR theory. The results of band-structure calculations by Kunz and Ginsberg<sup>9</sup> were used to aid in the choice of phase shifts for the scattering.

In Sec. IV we employ the scattering parameters used by Tsang and Ginsberg<sup>8</sup> to calculate the electromagnetic absorption in the SR model with three partial waves and compare this with the experimental results of Dick and Reif<sup>1</sup> for Pb-Mn films. Also included here are some predicted absorption curves for Zn-Mn alloys. This is preceded in Sec. II by an outline of the formalism used and a brief discussion of the calculation. Section III deals with some general observations on a structure in the ab-

sorption curves which is predicted to occur in SR theory at finite temperature.

### II. CALCULATION

In a previous paper on critical magnetic fields<sup>10</sup> we have discussed the solution of the Bardeen-Cooper-Schrieffer (BCS) equations with paramagnetic impurities in the SR model on the real frequency axis. The relevant equations are (3) and (4) of the paper:<sup>10</sup>

$$\Delta(\alpha, T) = N_0 V \int_0^{\omega_D} \text{Re} \left[ \frac{1}{[u^2(\omega) - 1]^{1/2}} \right] \tanh \left[ \frac{\beta\omega}{2} \right] d\omega, \quad (1)$$

$$\omega = u(\omega)\Delta(\alpha, T)$$

$$-i \frac{u(\omega)}{[u^2(\omega) - 1]^{1/2}} \sum_l (2l + 1) \alpha_l \left[ \frac{u^2(\omega) - 1}{u^2(\omega) - \epsilon_l^2} \right]. \quad (2)$$

Here  $N_0 V$  is the usual BCS coupling constant and  $\omega_D$  the cutoff frequency of the interaction. Also,  $\alpha_l = (n_I / 2\pi N_0)(1 - \epsilon_l^2)$ , where  $n_I$  is the paramagnetic impurity concentration,  $N_0$  is the single spin density of states at the Fermi level in the normal state, and  $\epsilon_l = \cos(\delta_l^+ - \delta_l^-)$ . The phase shifts  $\delta_l^{+(-)}$  are for the *l*th partial wave for spin-up (-down) electrons. As usual  $\beta = 1/k_B T$  where  $T$  is absolute temperature, and the function  $u(\omega) = \omega/\Delta(\omega)$  is simply related to the complex gap function  $\Delta(\omega)$ .

Once equations (1) and (2) have been solved self-consistently at a given temperature and impurity concentration for the order parameter  $\Delta(\alpha, T)$  and the complex function  $u(\omega)$ , the evaluation of the electromagnetic absorption for thin films is straightforward. The absorption is simply the real part of the frequency-dependent conductivity, which has been given by Nam<sup>11</sup> in terms of the complex gap function. Thus,

$$\frac{\sigma_1(\omega)}{\sigma_N} = \frac{1}{\omega} \int_{\omega_g - \omega}^{\omega_g} d\omega' [n(\omega')n(\omega + \omega') + p(\omega')p(\omega + \omega')] \tanh \left[ \frac{\beta}{2}(\omega + \omega') \right] + \frac{1}{\omega} \int_{\omega_g}^{\infty} d\omega' [n(\omega')n(\omega + \omega') + p(\omega')p(\omega + \omega')] \left[ \tanh \left[ \frac{\beta}{2}(\omega + \omega') \right] - \tanh \left[ \frac{\beta}{2}\omega' \right] \right]. \quad (3)$$

Here

$$n(\omega) = \text{Re}\{u(\omega)/[u^2(\omega) - 1]^{1/2}\}$$

is the single-particle density of states and

$$p(\omega) = \text{Re}\{1/[u^2(\omega) - 1]^{1/2}\}$$

is the pair density of states.  $\sigma_N$  is the normal-state conductivity, which is assumed to be frequency independent over the range of interest. The frequency  $\omega_g$  is the lowest frequency where the density of states becomes nonzero. Note that only the first integral in (3) contributes at zero temperature.

### III. ABSORPTION IN SR THEORY AT FINITE TEMPERATURE

Let us first review some well-known properties of electromagnetic absorption of superconductors. Recall that in BCS theory at zero temperature there is no absorption for  $\omega < 2\omega_g$ , where  $\omega_g = \Delta$ . At finite temperature there is some absorption at all frequencies, but for relatively low temperature ( $T/T_c \leq 0.2$ )  $\sigma_1(\omega)$  is negligibly small in the "gap" when compared with the absorption at higher frequencies. The absorption does increase at low frequencies, however, and diverges at zero frequency. The singular behavior at zero frequency arises from the square-root singularity in the density of states at  $\omega = \Delta$ . Qualitatively, one might say that some states above the Fermi level are thermally occupied, and these quasiparticles have an infinite density of states to scatter into with the absorption of a photon of vanishingly small energy.

With paramagnetic impurities in the AG model the situation is qualitatively very similar. At zero temperature there is no absorption for  $\omega < 2\omega_g$ , but in this case  $\omega_g < \Delta$ . In fact, as the impurity concentration increases  $\omega_g$  approaches zero (gapless region). At nonzero temperature there is finite absorption at all frequencies, with a peak at zero frequency. In contrast to the pure BCS case the peak at zero frequency is finite, which may be attributed to the disappearance of the singularity in the density of states with the addition of the paramagnetic impurities (see Nam<sup>11</sup>).

In SR theory the addition of regions of nonzero density of states within the gap results in extra structure in the zero-temperature absorption. This can be understood qualitatively by examining the density of states (Fig. 1). At finite temperature the same mechanism which is in-

involved in the AG case gives rise to a finite peak at zero frequency. Of more interest here is the appearance of what may be a large peak in the absorption at a frequency between  $\omega = 0$  and  $\omega = \Delta$ . This new peak appears at a frequency which does not necessarily coincide with any of the zero-temperature peaks and displays a more dramatic temperature dependence than the absorption at higher frequencies. Figure 2(a) shows one example of the behavior.

To help explain this effect recall Eq. (3) for the absorption in terms of the density of states:

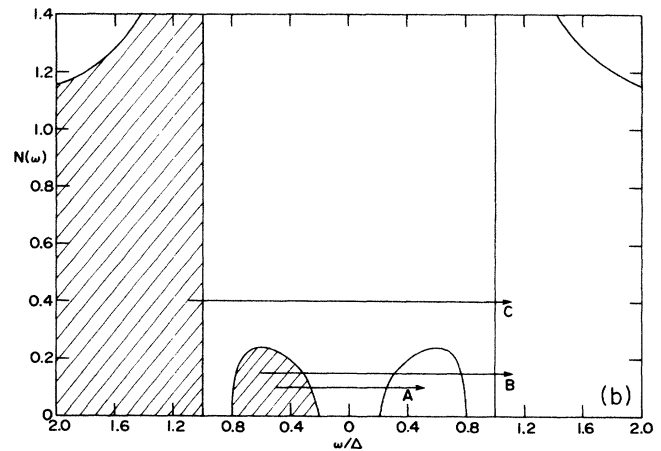
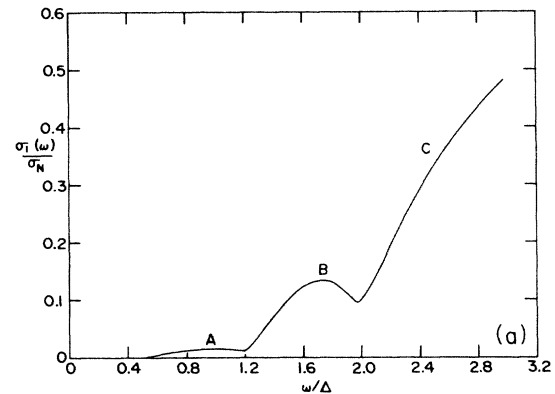


FIG. 1. (a) Typical electromagnetic absorption curve for a single phase shift ( $\epsilon_0 = 0.5$ ) for an impurity concentration ( $\alpha$ ) of 10% of the critical value ( $\alpha_c$ ) at  $T = 0$ . The features labeled  $A-C$  arise from the qualitatively distinct quasiparticle scattering processes indicated in (b). (b) Density of states  $N(\omega)/N_0$  for the same parameters as in (a). The arrows labeled  $A-C$  represents the quasiparticle scattering processes responsible for the similarly labeled features of the absorption curve in (a).

$$\frac{\sigma_1(\omega)}{\sigma_N} = \frac{1}{\omega} \int_{\omega_g - \omega}^{\omega_g} [n(\omega')n(\omega + \omega') + p(\omega')p(\omega + \omega')] \tanh \left[ \frac{\beta}{2}(\omega + \omega') \right] d\omega' \\ + \frac{2}{\omega} \int_{\omega_g}^{\infty} [n(\omega')n(\omega + \omega') + p(\omega')p(\omega + \omega')] \{f(\beta\omega')[1 - f(\beta(\omega + \omega'))] - f(\beta(\omega + \omega'))[1 - f(\beta\omega')]\} d\omega'. \quad (4)$$

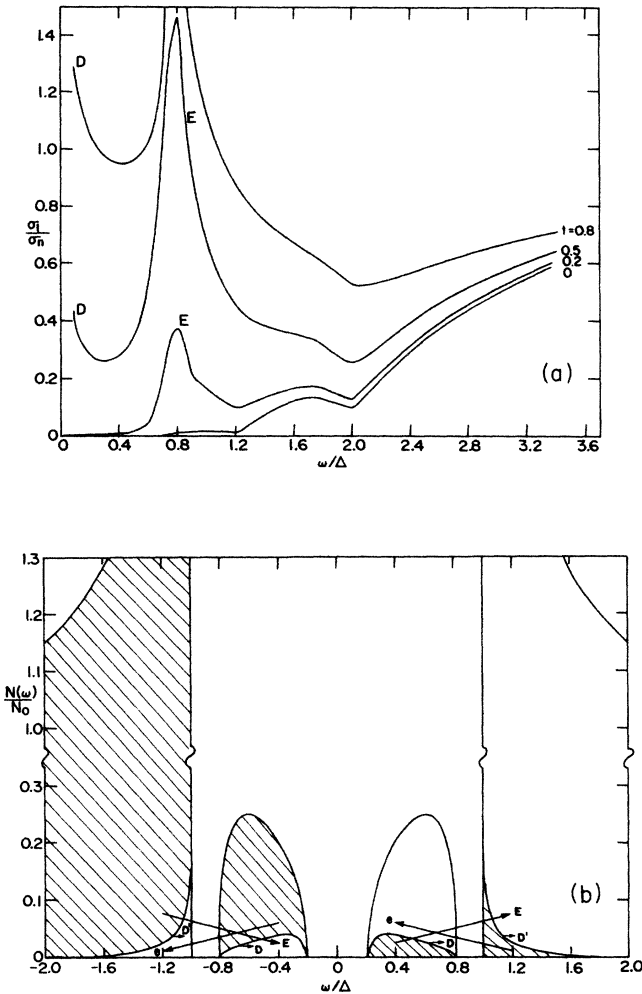


FIG. 2. (a) Electromagnetic absorption curves for the scattering parameter  $\epsilon_0=0.5$ , reduced impurity concentration  $\alpha/\alpha_c=0.1$ , and various temperatures. The curves are labeled by reduced temperature  $t=T/T_c$ . (b) Density of states  $N(\omega)/N_0$  for  $\epsilon_0=0.5$ ,  $\alpha/\alpha_c=0.1$ , and  $T/T_c=0.5$ . The shaded areas represent occupied states and the unshaded regions indicate unoccupied states. The arrows labeled  $D$  and  $D'$  represent the low-energy absorption processes which give rise to the peak at zero frequency labeled  $D$  in (a). The corresponding stimulated emission processes have not been indicated in order to minimize the clutter. The arrows labeled  $E$  represent the absorption processes and those labeled  $e$  the stimulated emission processes which lead to the peak in the absorption labeled  $E$  in (a). Of course events of the types labeled  $A-C$  in Fig. 1(b) also contribute at finite temperature.

The identity  $\tanh(x/2) = 1 - 2f(x)$  was used in rewriting the second integral in (4). Note that the first integral in (4) contributes at all temperatures, and does not change in a dramatic way on going from zero to finite temperature. It is the second integral which contributes only at nonzero temperatures which gives rise to the peak in question.

The second integral in (4) was written in this form to emphasize the similarity of tunneling  $I-V$  characteristics, and to allow qualitative identification of the various contributions. The first occupation factor  $f(\beta\omega')[1 - f(\beta(\omega + \omega'))]$  indicates absorption of a photon of frequency  $\omega$ , with a quasiparticle scattering from  $\omega'$  to  $\omega + \omega'$ . The subtracted term  $-f(\beta(\omega + \omega'))[1 - f(\beta\omega')]$  corresponds to stimulated emission of a photon  $\omega$ , with a quasiparticle dropping from  $\omega + \omega'$  to  $\omega'$ . The absorption will be maximized when the first contribution is large and the subtracted term is relatively small.

Figure 2(b) illustrates pictorially the qualitatively distinct scattering processes which contribute only at finite temperatures. The arrows labeled  $E$  represent the absorption processes and those labeled  $e$  the emission processes which give rise to the peak in question, labeled  $E$  in Fig. 2(a). If one looks in the positive energy region (above the Fermi level) of Fig. 2(b), one can see that while the number of occupied states in the impurity levels (roughly  $0.2 < \omega/\Delta < 0.8$ ) is comparable to the number of occupied states just above the main rise ( $1.0 < \omega/\Delta \leq 1.8$ ), this is not true for the unoccupied states. There are many more unoccupied states available above  $\omega/\Delta = 1.0$ , which means that the phase space for absorption events at  $\omega/\Delta \approx 0.8$  is much larger than that for stimulated emission. This results in strong absorption. For frequencies larger or smaller than the optimum value this unbalance between the phase space available for absorption and emission decreases, resulting in less net absorption.

In general, such a peak in the absorption can be expected to occur near the frequency  $\Delta - \omega_g$  as long as the impurity concentration is small enough so that a well-defined peak still exists in the density of states near  $\omega = \Delta$ . Note also that as the AG limit ( $\epsilon_0=1.0$ ) is approached this peak moves toward zero frequency and merges with the peak which always exists there.

#### IV. Mn ALLOYS

The electromagnetic absorption experiments of Dick and Reif<sup>1</sup> on Pb-Mn films have been examined in terms of SR theory by Machida.<sup>7</sup> He has found that the parameter  $\epsilon_0=0.5$ , close to the value  $\epsilon_0=0.55$  used by Chaba and

Nagi<sup>4</sup> to explain the tunneling conductance of Pb-Mn, gives significantly better agreement than does AG theory.

However, Tsang and Ginsberg<sup>8</sup> have performed tunneling experiments using dilute Pb-Mn alloys and have found that a single partial wave in SR theory cannot explain both the structure in the density of states and the magnitude of the depression of  $T_c$  relative to the critical temperature of pure Pb,  $T_c^0$ . They have analyzed their results in terms of two sets of parameters derived from band-structure calculations by Kunz and Ginsberg.<sup>9</sup> These values are the following: for parameter set I,  $\epsilon_0=0.985$ ,  $\epsilon_1=0.967$ , and  $\epsilon_2=0.970$ ; and for parameter set II,  $\epsilon_0=0.959$ ,  $\epsilon_1=-0.680$ , and  $\epsilon_2=0.990$ .

Figure 3 shows a comparison of some of the experimental results of Dick and Reif<sup>1</sup> with SR theory using these two sets of parameters. The calculated curves are finite-temperature results, using the experimental temperature

$T=1.5$  K. The curves for parameter set I in Fig. 3(a) differ significantly from the experimental results. There is simply too much absorption at low frequencies to be explained by these parameters. Note that these calculated curves are very similar in shape to the AG results because all of the scattering parameters ( $\epsilon_i$ 's) are quite near 1.0.

On the other hand, the fit with parameter set II in Fig. 3(b) is much better, roughly the same as Machida<sup>7</sup> has found using the single scattering parameter  $\epsilon_0=0.5$ . However, it should be noted that there still remains a significant discrepancy between theory and experiment for the lower-frequency region of the low-concentration curves. There seems to be more absorption at low frequencies than is predicted for these parameters. While a different choice of parameters could improve the fit here, it could only serve to worsen this agreement for the higher Mn concentrations where the fit is reasonably good now. The origin of this problem is still unclear.

It should be mentioned that approximate strong-coupling corrections have been made by using the equation

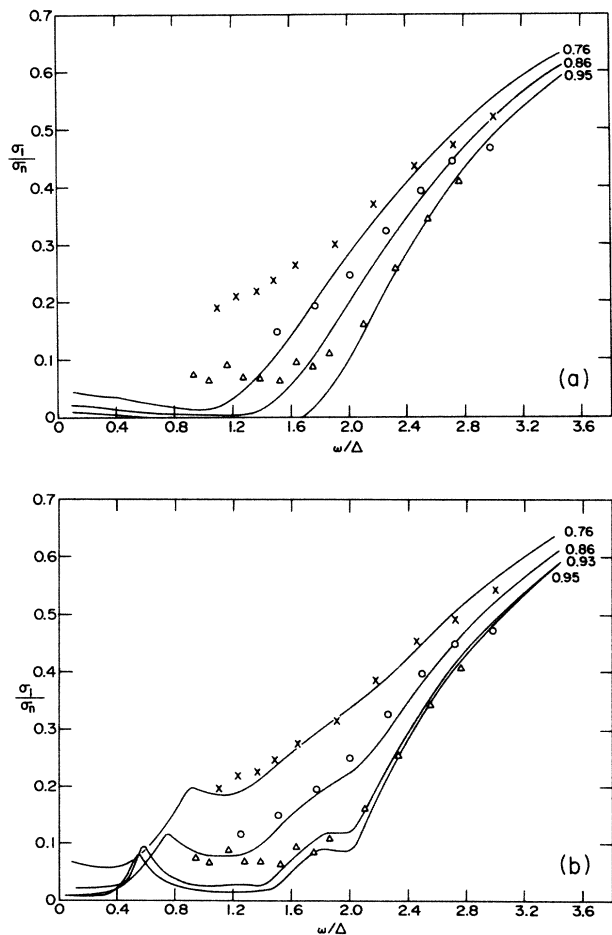


FIG. 3. The electromagnetic absorption for two models of Pb-Mn alloys. The curves are labeled by reduced critical temperature  $T_c/T_c^0$  and are all for an absolute temperature of  $T=1.5$  K. The experimental points are due to Dick and Reif (Ref. 1), and were rescaled as described in Sec. IV. (a) Scattering parameter set I:  $\epsilon_0=0.985$ ,  $\epsilon_1=0.967$ , and  $\epsilon_2=0.970$ . (b) Scattering parameter set II:  $\epsilon_0=0.959$ ,  $\epsilon_1=-0.680$ , and  $\epsilon_2=0.990$ .

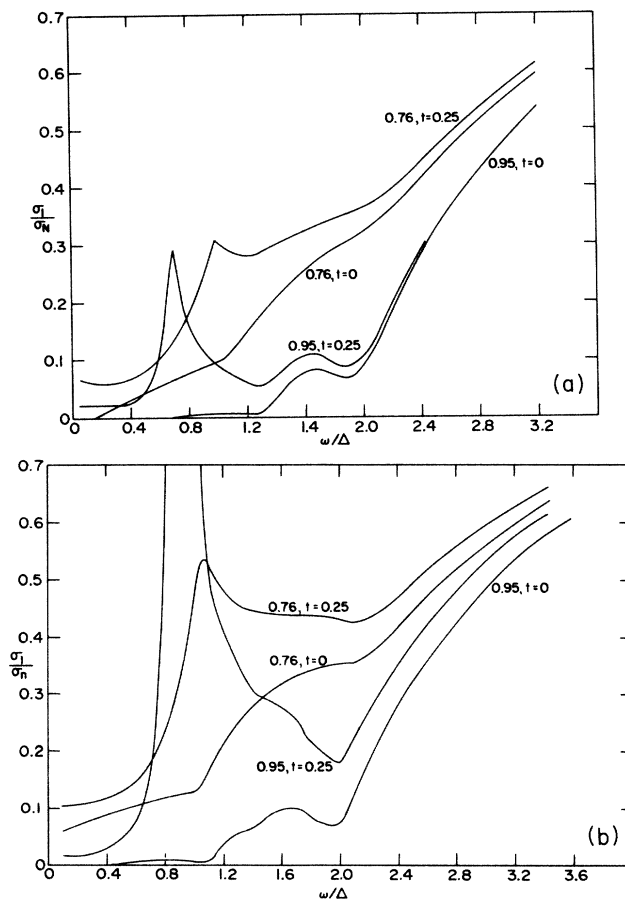


FIG. 4. The electromagnetic absorption for two models of Zn-Mn alloys. The curves are labeled by reduced critical temperature  $T_c/T_c^0$  and reduced temperature  $t=T/T_c$ . (a) Scattering parameter set Zn-Mn I:  $\epsilon_0=1.0$ ,  $\epsilon_1=0.53$ , and  $\epsilon_2=0.94$ . (b) Scattering parameter set Zn-Mn II:  $\epsilon_0=0.25$ ,  $\epsilon_1=0.50$ , and  $\epsilon_2=1.0$ .

$$\frac{\omega}{\Delta} = \frac{\omega}{T_c^0} \left( \frac{T_c^0}{\Delta_0} \right) \left( \frac{\Delta_0}{\Delta} \right)$$

to manipulate the data of Dick and Reif.<sup>1</sup> Here the experimental value of  $\Delta_0/T_c^0=2.31$  has been used, along with the ratio  $\Delta/\Delta_0$  determined from our weak-coupling calculation. Also, because the absolute value of  $\sigma_1/\sigma_N$  was not experimentally determined, the normalization of this axis is somewhat model dependent. We have simply adjusted this so that the last few points are close to the theoretical curves.

Although no electromagnetic absorption results for Zn-Mn are available in the literature, we show some predicted curves in Fig. 4. The scattering parameters used are due to Terris and Ginsberg,<sup>12</sup> who analyzed tunneling experiments on Zn-Mn alloys in terms of three partial waves in SR theory. We<sup>10</sup> have previously used their parameters to calculate critical magnetic fields for these alloys. The two sets of parameters are as follows: for Zn-Mn I,  $\epsilon_0=1.00$ ,  $\epsilon_1=0.53$ , and  $\epsilon_2=0.94$ ; and for Zn-Mn II,  $\epsilon_0=0.25$ ,  $\epsilon_1=0.50$ , and  $\epsilon_2=1.00$ .

While the zero-temperature curves in Figs. 4(a) and 4(b) do differ significantly, the overall shapes are similar and it could be difficult to choose between them experimentally. However, the markedly different calculated temperature dependence for the two different parameter sets could be useful in establishing which set better describes real Zn-Mn alloys. One other point which bears mentioning is that the weak-coupling nature of Zn alloys makes these results directly comparable with experiments. In the case of Pb alloys, one must be more careful in applying results of BCS calculations because of possible strong-coupling corrections.

## V. CONCLUSIONS

We have calculated the electromagnetic absorption for thin-film superconducting alloys in the SR model. A significant extra peak is found at finite temperature, which can be attributed to quasiparticle scattering from the band of states in the gap to above the gap edge (with the converse contribution from below the Fermi level). The temperature dependence of this peak varies with the choice of scattering parameters, so this may be useful in helping to determine appropriate parameters for a given alloy.

Using parameters previously used by Tsang and Ginsberg<sup>8</sup> to explain the tunneling conductance of Pb-Mn alloys, the absorption of Pb-Mn films has been calculated and compared with the experiment of Dick and Reif.<sup>1</sup> Whereas the tunneling experiments of Tsang and Ginsberg<sup>8</sup> do not rule out one parameter set or the other, our results show that parameter set I ( $\epsilon_0=0.985$ ,  $\epsilon_1=0.967$ ,  $\epsilon_2=0.970$ ) is incompatible with the measured absorption. The parameter set II ( $\epsilon_0=0.959$ ,  $\epsilon_1=-0.680$ , and  $\epsilon_2=0.990$ ) is found to be reasonably consistent with the experiment data.

Some predictions have also been made for the electromagnetic absorption of Zn-Mn alloys. Two different sets of parameters which give roughly similar fits to the tunneling conductance are found to give significantly different absorption curves. In summary, one can conclude that electromagnetic absorption measurements may be very useful in combination with tunneling results to aid in the determination of scattering parameters in SR models of superconducting alloys.

## ACKNOWLEDGMENTS

This research was supported by the Natural Sciences and Engineering Research Council of Canada (NSERC).

<sup>1</sup>G. J. Dick and F. Reif, *Phys. Rev.* **181**, 774 (1969).  
<sup>2</sup>A. A. Abrikosov and L. P. Gor'kov, *Zh. Eksp. Teor. Fiz.* **39**, 1781 (1960) [*Sov. Phys.—JETP* **12**, 1243 (1961)].  
<sup>3</sup>M. A. Woolf and F. Reif, *Phys. Rev.* **137**, A557 (1965).  
<sup>4</sup>A. N. Chaba and A. D. S. Nagi, *Nuovo Cimento Lett.* **4**, 794 (1972).  
<sup>5</sup>H. Shiba, *Prog. Theor. Phys.* **40**, 435 (1968).  
<sup>6</sup>A. I. Rusinov, *Zh. Eksp. Teor. Fiz.* **56**, 2043 (1969) [*Sov.*

*Phys.—JETP* **29**, 1101 (1969)].  
<sup>7</sup>K. Machida, *Prog. Theor. Phys.* **54**, 1251 (1975).  
<sup>8</sup>J. K. Tsang and D. M. Ginsberg, *Phys. Rev. B* **22**, 4280 (1980).  
<sup>9</sup>A. B. Kunz and D. M. Ginsberg, *Phys. Rev. B* **22**, 3165 (1980).  
<sup>10</sup>W. Stephan and J. P. Carbotte, *Phys. Rev. B* **31**, 2952 (1985).  
<sup>11</sup>S. B. Nam, *Phys. Rev.* **156**, 487 (1967).  
<sup>12</sup>B. D. Terris and D. M. Ginsberg, *Phys. Rev. B* **29**, 2503 (1984).